RESEARCH ARTICLE

Changes in soil properties and resistance to concentrated flow across a 25-year passive restoration chronosequence of grasslands on the Chinese Loess Plateau

Ming-Ming Guo[1] , Wen-Long Wang[1,2,3], Hong-Liang Kang[1], Bo Yang[1], Jian-Ming Li[2,4]

Revegetation represents an effective measure for preventing soil erosion on the Loess Plateau. However, the effects of revegetation-induced changes in soil and root properties on soil resistance to concentrated flow erosion (SRC) remain unclear. This study sampled soils and roots across a 25-year chronosequence from farmland to grasslands of different ages (3, 7, 10, 18, and 25 years) to quantify variations in soil and root properties (soil bulk density, SBD; soil disintegration rate, SDR; saturated hydraulic conductivity, SHC; organic matter content, OMC; water-stable aggregate, WSA; mean weight diameter, MWD; root mass density, RMD; root length density, RLD; and root surface area density, RSAD) and their effects on SRC. Farmland and grassland SRCs were obtained using a hydraulic flume. Soil properties and root density gradually improved with restoration time. In terms of the comprehensive soil property index calculated via principal component analysis, grassland values were 0.66 to 1.94 times greater than farmland values. Grassland SRCs increased and gradually stabilized (>18 years) over time and were 1.60 to 8.26 times greater than farmland SRC. SRC improvement was significantly related to increases in OMC, SHC, WSA, and MWD and decreases in SBD and SDR over time. SRC was effectively simulated by the Hill curve of RMD, RLD, and RSAD. SDR, SHC, and RMD (0.5–1.0 mm) affected SRC the most. This study scientifically describes how revegetation improves soil quality and soil resistance to flow erosion, and suggests that vegetations rich in 0.5–1.0 mm roots should be preferred during revegetation.

Key words: Chinese Loess Plateau, root density, soil erodibility, soil quality, vegetation restoration

Implications for Practice

- Revegetation should be considered an effective and important approach for improving soil quality and soil erosion resistance on the Loess Plateau.
- Plants with more fine roots and high root density should be used in restoration.
- Within the first 18 years following passive restoration, the soil quality and soil resistance of grasslands gradually stabilize.
- Restoration practices need to pay attention to two points: first, an appropriate grass root density can greatly improve soil quality and resistance; second, reduced water consumption of grasses may be preferred due to the lack of soil moisture on the Loess Plateau.

Introduction

The Chinese Loess Plateau is widely acknowledged to have some of the most severe soil and water loss worldwide (Li & Shao 2006), with mean annual soil erosion rates ranging from 5,000 to 10,000 t km^{-2} yr^{-1} (Wang et al. 2014). To control soil erosion and restore ecosystems, China launched the "Grain for Green" project in 1999, which aims to restore degraded cropland

to forest and grassland (Fu et al. 2000). Since the project was implemented, soil loss rates on slopes of 8°–35° have decreased from 5,000–8,500 to 3,600–5,500 t km^{-2} yr^{-1} in 2010 (Fu et al. 2011). Vegetation restoration has been proven to be an effective approach for reducing soil erosion because of its importance in improving soil erosion resistance (Fu et al. 2011; Wang et al. 2014).

Previous studies documented that the improvement in soil resistance to concentrated flow erosion is closely related to root

system and its effect on soil properties (Gyssels & Poesen 2010; Vannoppen et al. 2015; Wang et al. 2015). Roots embed in the soil body and form a soil–root matrix, thereby reinforcing soil ability to resist erosion (Li et al. 2017; Wang & Zhang 2017). In addition, diverse root exudates adhere to soil particles and enhance the bonding power between soil particles and roots (Zhu et al. 2010; Zhao et al. 2013). Wang et al. (2015) determined that root bonding can account for greater than 25% of the soil loss reduction caused by roots. Moreover, many studies have investigated the relationships between soil resistance and root characteristics. Li et al. (1992) reported that the enhancement of soil anti-scourability is positively related to the number of fine roots (diameter < 1 mm). However, Mamo and Bubenzer (2001) noted that root length density (RLD) had a closer relationship with soil resistance to concentrated flow. Additionally, soil resistance also has a close relationship with root morphology and structure (De Baets et al. 2007; Wang & Zhang 2017). Wang and Zhang (2017) revealed that soil detachment capacity of grasslands with tap roots was 14.7 times greater than that of grasslands dominated by species with fibrous roots.

Root exudates also influence soil properties and further change soil resistance to concentrated flow erosion. Previous studies have shown that root systems can optimize soil porosity structure (Li & Shao 2006; Wu et al. 2016), improve soil infiltration capacity (Hu et al. 2009; Zhao et al. 2013), strengthen water-stable aggregate (WSA) stability and soil cohesion (Li & Shao 2006; Wang et al. 2014), and increase soil organic matter (Wang et al. 2014; Guo et al. 2018), nutrients (Peichl et al. 2012), and soil microorganism species (Zhu et al. 2010). Moreover, the improvement of soil properties induced by revegetation has been linked to improved soil resistance (Li et al. 2017; Guo et al. 2018). For example, Zhou et al. (2010) and Li et al. (2015, 2017) reported that soil resistance to concentrated flow was negatively correlated with soil bulk density (SBD) and soil disintegration rate (SDR) and positively correlated with soil infiltration rate and WSAs.

In the past several decades, significant advances have been made in quantifying the relationship between soil resistance to concentrated flow erosion and soil and root properties. However, the effects of changes in soil properties caused by vegetation succession on soil resistance remain unclear. During revegetation, different vegetation communities cause different changes in soil properties, albeit in the same region with similar growth environments (Jiao et al. 2010; Guo et al. 2018; Wang et al. 2018). Since the 1970s, a series of ecological restoration projects have been conducted to control soil and water loss on the Loess Plateau. Slope farmland (SF) areas diminished by 43% between 1984 and 1996, whereas forest and grassland areas increased by 36 and 5%, respectively (Fu et al. 2000). With the implementation of the Grain for Green Project in 1999, grassland area (2.6×10^5 km^2) accounted for 41.7% of the Loess Plateau in 2010 (Li et al. 2016). Grassland plays an important role in soil and water conservation in this region, while the grassland succession process and its corresponding dominant community have differed greatly in different regions due to large differences in climate, seed bank source, and topographic conditions, etc. (Jiao et al. 2008; Kou et al. 2016). Thus, soil and root properties greatly change with successional time, and the varied soil and root properties are also expected to influence soil resistance to concentrated flow erosion.

Therefore, to better evaluate the impacts of revegetation on soil properties and resistance to concentrated flow erosion over time, we assumed that soils from five farmlands before restoration had similar spatial textural homogeneity and followed similar underlying mechanisms during restoration. The objective of this study was to (1) explore how soil and root properties and soil resistance to concentrated flow change with successional time; (2) determine how soil and root properties affect soil resistance to concentrated flow erosion; and (3) identify which root diameters have the optimal effect on improving soil resistance.

Methods

Study Area and Sampling Site Selection

This study was conducted in the Nanxiaohegou watershed (35°41′N to 35°44′N, 107°30′E to 107°37′E; 1,050–1,423 m elevation; 36.3 km^2; Fig. 1), Qingyang City, China. The study area is a typical loess tableland-gully region and is characterized by a temperate continental semiarid climate (Liang et al. 2010). The annual mean temperature is 10°C, and the frost-free period is 160–180 days. Annual precipitation is approximately 523 mm, with 58.8% of the total precipitation occurring between July and September in the form of short heavy rain storms (Guo et al. 2018). Major soil types are loessial soils. Since the 1970s, soil and water losses have been controlled effectively by a series of soil and water conservation projects, such as the Three Protection Belts Model, the Four Eco-economical Belts Model, and the Grain for Green Project (Zhao 1994; Li et al. 2016). The vegetation communities contain mainly planted trees and shrubs and native secondary herbaceous plants.

Based on a detailed field survey and previous research outcomes on passive vegetation successional patterns in the study area (Liang et al. 2010), grasslands with five restoration ages (3, 7, 10, 18, and 25 years) across a chronosequence of passive succession were selected in this watershed (Fig. 1). The five farmlands before restoration were planted with the same crop types and experienced similar tillage and fertilization practices. Thus, soils of the five farmlands had similar spatial textural homogeneity and followed similar underlying mechanisms during restoration. In addition, slope aspect and gradient, elevation, and soil type of the five selected sites were similar to minimize the effects of these factors. For comparison, one corn-planted sloping farmland site, with topography similar to that of the grasslands, was selected as a control. Basic characteristics of the six selected sites are summarized in Table 1.

Soil Sampling and Laboratory Analysis

This study was conducted from July to September 2018, when vegetation growth and biomass are at their maximum over the course of a year. Moreover, soil erosion is the most
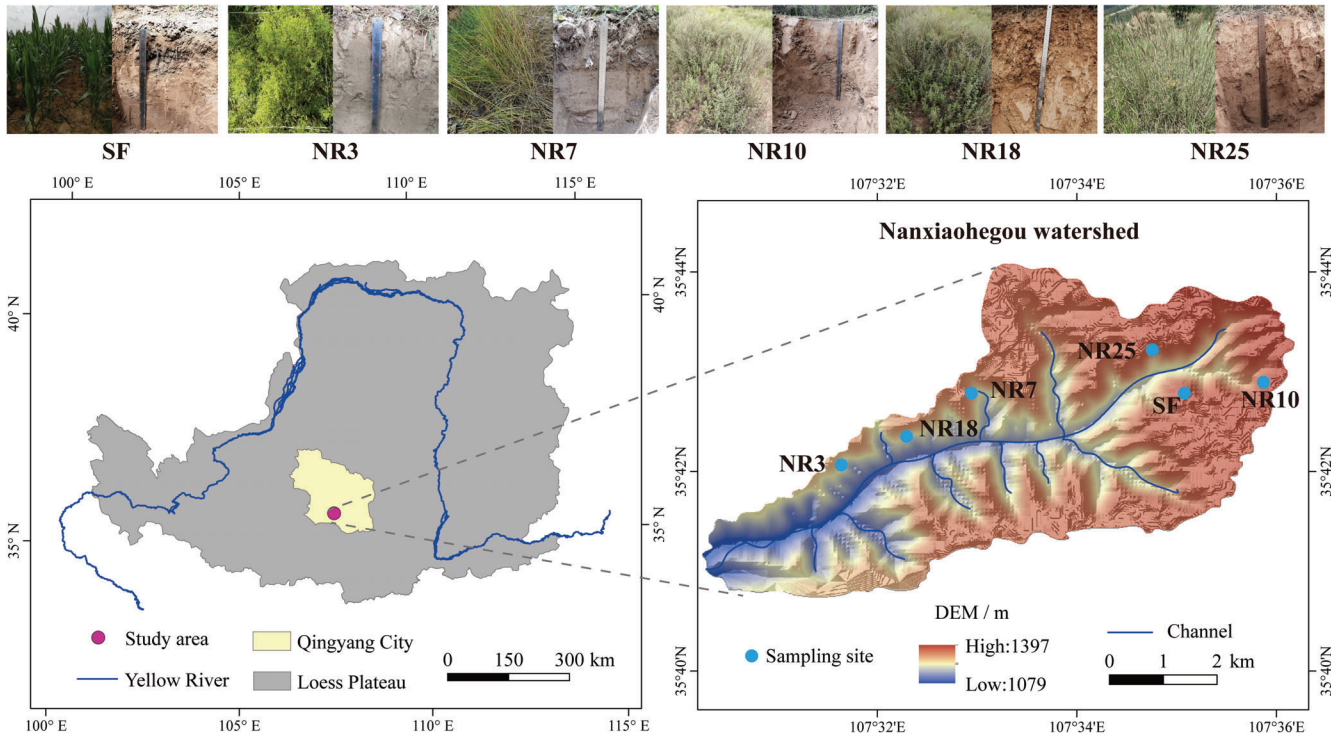
Figure 1. Location of the study area in the Loess Plateau, position of sampling sites in the Nanxiaohegou watershed, and photographs of the plants and soil profiles (0–50 cm) at each sampling site. SF refers to slope farmland. NR3, NR7, NR10, NR18, and NR25 represent 3, 7, 10, 18, and 25 years, respectively, of passive restoration.

Table 1. Basic characteristics of the six selected sampling sites. SF represents slope farmland. NR3, NR7, NR10, NR18, and NR25 represent 3, 7, 10, 18, and 25 years of passive restoration, respectively.

	Site Code					
	SF	*NR3*	*NR7*	*NR10*	*NR18*	*NR25*
Restoration time (yr)	0	3	7	10	18	25
Slope (%)	25.86	25.30	30.19	29.24	25.56	24.74
Vegetation cover (%)	—	62.3	72.1	80.8	83.4	91.2
Altitude (m)	1,270	1,255	1,260	1,261	1,240	1,232
Vegetation-dominant species	*Zea mays*	*Artemisia scoparia*	*Agropyron cristatum*	*Artemisia sacrorum*	*Artemisia sacrorum*	*Bothriochloa ischaemum*
Sand (>0.02 mm) (%)	14.86	15.65	15.88	16.14	15.17	16.63
Silt (0.02–0.002 mm) (%)	73.17	74.04	73.08	72.87	73.82	73.02
Clay (<0.002 mm) (%)	11.97	10.31	11.05	10.99	11.02	10.35

serious during this period. Therefore, studying soil resistance to concentrated flow erosion in this period is the most realistic. Four replicated quadrats (5 m × 5 m) were set from top to bottom along the hillslope of each site for sampling. Soil samples were collected from topsoil (0–20 cm) with the litter layer removed because grass roots are mainly distributed in topsoil (Li et al. 2005). In each quadrat, five samples were collected using steel rings (200 cm³) in random sampling method to form a composite sample, and a total of 24 composite samples were used to determine soil organic matter content (OMC), particle size distribution (PSD), and WSA greater than 0.25 mm. The potassium dichromate external heating method was used to measure OMC (Zhu et al. 2010). Soil PSD was measured with a Master-Sizer 2000 laser sizer (Malvern Instruments Ltd., Malvern, U.K.). Sieves with apertures (0.25, 0.5, 1.0, 2.5, and 5.0 mm) were used to determine WSA (Wang et al. 2014). Six soil samples were obtained in each quadrat with a steel cutting ring (200 cm³), and a total of 144 samples (six sites × four quadrats × six samples) were analyzed to determine SBD using an oven-drying method at 105°C for 24 hours and saturated hydraulic conductivity (SHC) using the constant water head test (Guo et al. 2018). SDR represents the weight of soil particles dissipated in static water per unit time, and three samples were collected with a square steel box (5 cm × 5 cm × 5 cm) in each quadrat to obtain SDR using a soil disintegrator (Jiang et al. 1995; Li et al. 2015; Guo et al. 2018).
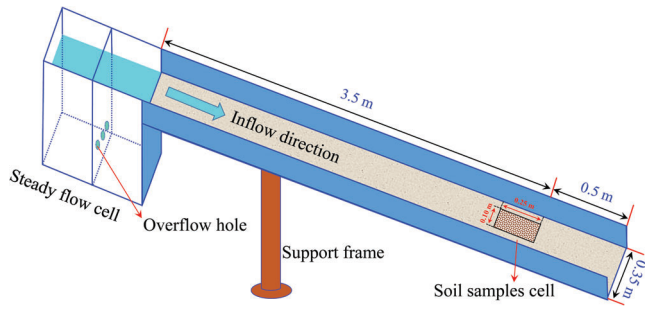
Figure 2. Schematic diagram of hydraulic scouring flume.

Undisturbed soils were sampled to determine soil resistance to concentrated flow erosion (Li et al. 2015; Zhang et al. 2017). First, the surface withered leaves were removed, and random sampling method was used to take the undisturbed soil sample with a steel sampling box (10 cm × 10 cm × 25 cm, depth × width × length). Then, the top and bottom ends of the undisturbed soil in the sampler were flattened, and both ends were covered with cotton cushions and lids to avoid disturbance during sample transport (Zhou et al. 2010; Li et al. 2017). A total of 72 samples (6 sites × 4 quadrats × 3 samples) were collected.

Test for Soil Resistance to Concentrated Flow Erosion

The 72 undisturbed soil samples were saturated for 12 hours in a container with a water level of 1 cm below topsoil surface and then drained for 12 hours (Zhang et al. 2017). Soil resistance to concentrated flow erosion was tested in a hydraulic flume that was 4 m long, 0.35 m wide, and 0.17 m deep (Fig. 2). The flume was long enough for water to steadily flow along the soil surface and wide enough to weaken the flume boundary effect on flow (Zhang 2017). A thin layer of paint was sprayed on the flume surface and sidewall to increase hydraulic roughness. Sand particles passed through a 1 mm sieve were pasted to the wet paint as evenly as possible (Zhang et al. 2017). A rectangular opening with same size as the sampling box was set as a 0.5 m section from flume bottom to ensure that the soil surface of the sampling box was at the same level as the flume surface. The flow rate and scouring time were set to 16 L/minutes and 15 minutes, respectively, according to the maximum runoff discharge and time frequency caused by a typical rainstorm on standard runoff plots (20 m × 5 m) in the study area (Li et al. 2015; Zhang et al. 2017). For each test, runoff and sediment samples were collected with sampling tanks at 1-minute intervals, and the sampling time was recorded. These sediment samples were oven-dried at 105°C for 24 hours to determine soil loss.

After the scouring test, roots were immediately separated from the sampling box by the washing method (De Baets et al. 2006; Yu et al. 2014). First, soil samples in the box were soaked in tap water for 1 hour to increase soil dispersion and then were placed on a 0.25 mm sieve and washed with tap water using a low-pressure head. The living roots, plant debris, and some pebbles were left on the sieve. Only the living roots were removed individually using tweezers (Yu et al. 2014). Washed roots

were divided into four root diameter classes (0–0.5, 0.5–1.0, 1.0–2.0, and 2.0–5.0 mm) using Vernier calipers. These roots were scanned using an Epson V700 scanner (Seiko Epson Corporation, Bandung, Indonesia) at a resolution of 300 dpi. Root characteristics were measured using Win RHIZO image analysis software (version 2007 pro) to obtain RLD (cm/cm^3) and root surface area density (RSAD, cm^2/cm^3). Then, the scanned roots were oven-dried for 24 hours at 65°C and weighed to calculate root mass density (RMD, kg/m^3).

Parameter Calculation and Statistical Analysis

Aggregate Mean Weight Diameter. WSA stability can be characterized by the value of the mean weight diameter (MWD), which was calculated as follows:

$$\text{MWD} = \frac{\sum_1^n (\overline{R}_i w_i)}{\sum_1^n w_i} \tag{1}$$

where $\overline{R}_i$ and w_i are the mean diameter of the i-class aggregate and the mass percent of i class, respectively.

Comprehensive Soil Property Index. Using a single soil property indicator to evaluate soil quality at different restoration times can lead to one-sided results. Therefore, the comprehensive soil property index (SPI), a comprehensive parameter based on principal component analysis (PCA) that comprehensively integrates various soil properties, was employed to evaluate the quality of soil properties. The SPI was calculated as follows:

$$\begin{pmatrix} \text{SPI}_1 \\ \text{SPI}_2 \\ \vdots \\ \text{SPI}_m \end{pmatrix} = Z \cdot \begin{pmatrix} F_1 \\ F_2 \\ \vdots \\ F_p \end{pmatrix} \tag{2}$$

$$Z = X \cdot Y = \begin{pmatrix} X_{1,1} & X_{1,2} & \cdots & \cdots & X_{1,n} \\ X_{2,1} & X_{2,2} & \cdots & \cdots & X_{2,n} \\ \cdots & \cdots & \cdots & \cdots & \cdots \\ \cdots & \cdots & \cdots & \cdots & \cdots \\ X_{m,1} & X_{m,2} & \cdots & \cdots & X_{m,n} \end{pmatrix}$$

$$\cdot \begin{pmatrix} \lambda_{1,1} & \lambda_{1,2} & \cdots & \cdots & \lambda_{1,p} \\ \lambda_{2,1} & \lambda_{2,2} & \cdots & \cdots & \lambda_{2,p} \\ \cdots & \cdots & \cdots & \cdots & \cdots \\ \cdots & \cdots & \cdots & \cdots & \cdots \\ \lambda_{n,1} & \lambda_{m,2} & \cdots & \cdots & \lambda_{n,p} \end{pmatrix} \tag{3}$$

where SPI_m is the SPI value of the m sample site, $m = 1, 2, 3, \ldots, 24$; F_p is the weight of the p principal component, $p = 1, 2, 3$ and $n = 1, 2, 3, \ldots, 9$; X is the standardized soil properties matrix; and Y is the eigenvector matrix of principal components. A higher SPI correlates to higher quality soil properties.

Soil Resistance Coefficient. Previous studies suggested that the soil resistance coefficient (SRC, L/g) can represent the soil
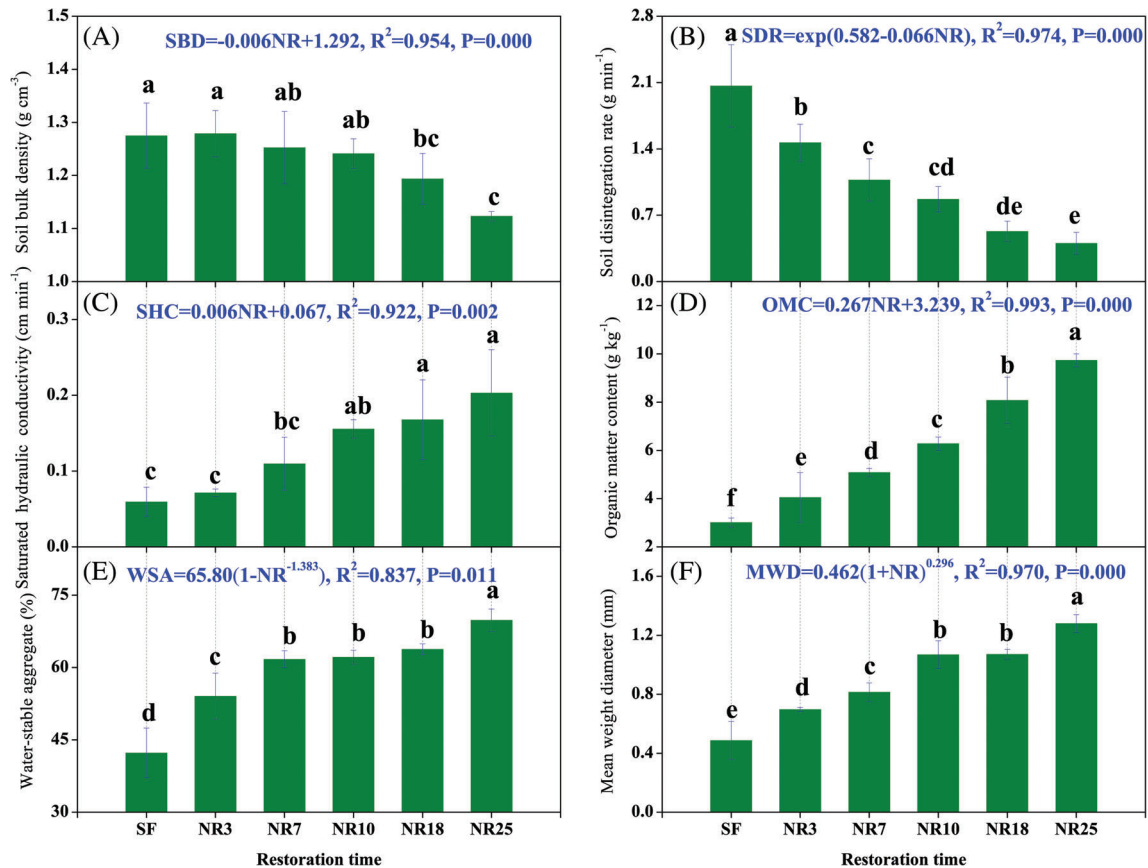
Figure 3. Variation in soil properties with restoration time. (A) Soil bulk density, (B) soil disintegration rate, (C) saturated hydraulic conductivity, (D) organic matter content, (E) water-stable aggregate, and (F) mean weight diameter. SF refers to slope farmland. NR3, NR7, NR10, NR18, and NR25 represent 3, 7, 10, 18, and 25 years, respectively, of passive restoration. Different lowercase letters in a figure indicate a significant difference among different restoration times ($p < 0.05$). Error bars represent ±SE.

resistance to concentrated flow erosion (Li et al. 2015; Zhang et al. 2017). The SRC is calculated as follows:

$$\mathrm{SRC} = \frac{q \cdot T}{M} \qquad (4)$$

where q is the flow rate (L/minutes), T is the experimental period (minutes), and M is the sediment dry weight of each test (g). A greater SRC value indicates a higher soil resistance.

Relationship Between SRC and Root Density. Theoretically, SRC could be considered zero when root density is infinitely close to zero and reaches a maximum value when root density reaches infinity. The Hill curve satisfies the change trend and was also widely employed to determine the relationships between soil resistance to concentrated flow and root density (De Baets et al. 2006; Vannoppen et al. 2015). Therefore, the Hill curve was selected to simulate the relationships between SRC and the root density of different root diameters and is expressed as follows:

$$\mathrm{SRC} = K\frac{X_r^a}{X_r^a + b} \quad (K > 0, a > 0, b > 0) \qquad (5)$$

where X_r represents root density parameters and K, a, and b are constants. K is the maximum value of SRC for infinite X_r. Additionally, the Hill curve can be used to evaluate the ability of roots to increase the resistance to concentrated flow based on the value of $b^{\wedge}(1/a)$. When the value of X_r is $b^{\wedge}(1/a)$, the SRC is improved by 50% (Li et al. 1991). In this study, $b^{\wedge}(1/a)$ can be used as an index to compare the effectiveness of different root diameters in improving soil SRC: a lower $b^{\wedge}(1/a)$ value corresponds to more effective roots.

Statistical Analyses and Figure Plotting. A one-way analysis of variance was performed to analyze differences in soil properties, root characteristics, and SRC among different restoration times. A PCA was performed to determine the overall differentiation of soil properties among six restoration times. A simple regression analysis was employed to analyze the relationships between SRC and soil properties. A stepwise regression analysis and path analysis were used to examine the effects of soil and root properties on the SRC (Wang et al. 2017). All statistical analyses were carried out with SPSS 16.0, and all figures were processed in R version 3.5.1 and Origin 8.5.

Results

Soil Properties

Soil properties significantly changed during vegetation succession ($p < 0.05$, Fig. 3). SBD did not change in the first 3 years and then significantly increased by 10.5–13.9% (7–25 years) compared with SF. Overall, the SBD linearly increased with restoration time (Fig. 3A, $p < 0.001$). SDR showed a significant decrease in the first 10 years ($p < 0.05$) and gradually stabilized (>18 years) (Fig. 3B). The SDRs in grasslands were 29.1–65.1% less than that in SF and exponentially decreased with increasing restoration time ($p < 0.001$). Soil SHC did not change in the first 7 years. However, after a 7-year restoration, the SHC of grasslands significantly increased ($p < 0.05$, Fig. 3C), and a linear function can describe the trend of SHC with restoration time ($p = 0.002$). With an increase in restoration time, plant roots and litter accumulated in soil and transformed gradually into organic matter. As a result, soil OMC in restored grasslands was significantly greater than that in SF by 0.34–2.23 times ($p < 0.05$, Fig. 3D) and linearly increased with restoration time ($p < 0.001$). Soil WSA greater than 0.25 mm and MWD significantly increased in the first 7 years, and then did not change over 10–18 years, while the WSA and MWD of 25-year grassland increased significantly by 9.4 and 19.5%, respectively (Fig. 3E & 3F). Furthermore, WSA and MWD increased as power functions with increasing restoration time ($p < 0.05$).

Linkages Between Vegetation Restoration and Soil Properties

A PCA was performed to study the effect of restoration time on soil properties. The ordination of the PCA (Fig. 4A) showed clear differences in soil properties among different restoration times. Sampling sites for soil properties were clustered into five groups differentiated by restoration time. The first group only contained SF, the second group included NR3, the third group included NR7 and NR10, the fourth included NR18, and the fifth group included NR25. The PCA revealed that the first two and first three principal components explained 76.4 and 89.9% (PC1 = 59.6%, PC2 = 16.8%, PC3 = 13.5%) of the total variance, respectively (Table 2), indicating that the first three principal components could express most of soil property
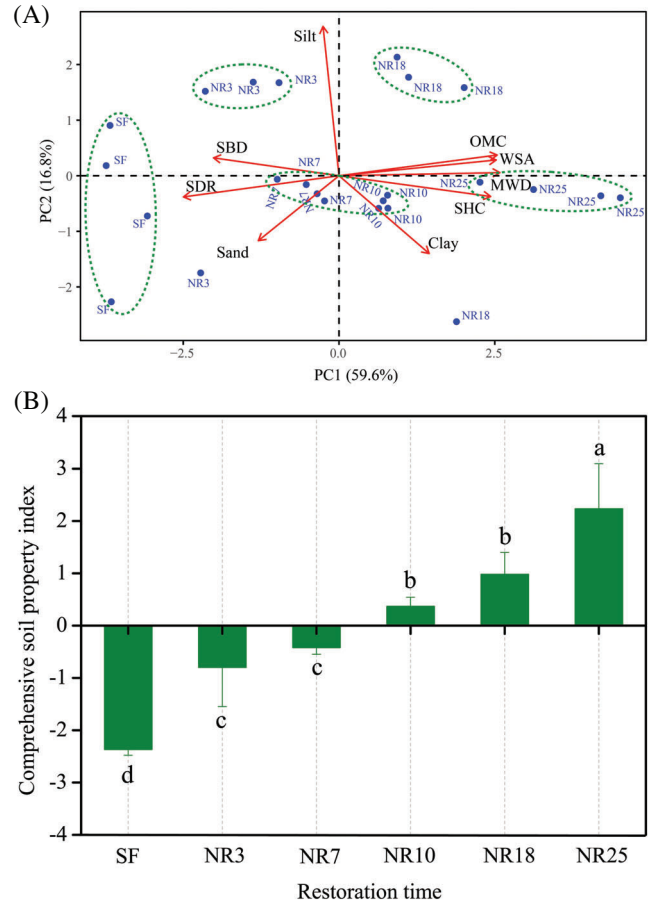

Figure 4. Results of principal component analysis (PCA) (A) and the comprehensive soil property index (B). SF refers to slope farmland. NR3, NR7, NR10, NR18, and NR25 represent 3, 7, 10, 18, and 25 years, respectively, of passive restoration. SBD, SDR, SHC, OMC, WSA, and MWD represent soil bulk density, soil disintegration rate, saturated hydraulic conductivity, organic matter content, water-stable aggregate, and mean weight diameter. Different lowercase letters indicate a significant difference among different restoration times ($p < 0.05$). Error bars represent ±SE.

information. The SHC, OMC, MWD, WSA, and clay content had positive weights on PC1, whereas SBD and SDR had negative weights (Fig. 4A), and the contributions of SDR, SHC,

Table 2. Total variance explained and principal component matrix of the principal component analysis.

| Component	Eigen-value	Variance (%)	Cumulative variance (%)	Component Matrix								
				Soil bulk density	Soil disintegration rate	Saturated hydraulic conductivity	Organic matter content	Water-stable aggregate	Mean weight diameter	Clay content	Silt content	Sand content
First principal component	5.37	59.62	59.66	−0.74	−0.92	0.90	0.94	0.93	0.95	0.53	−0.09	−0.48
Second principal component	1.51	16.81	76.44	0.12	−0.14	−0.14	0.14	0.10	0.02	−0.51	0.99	−0.43
Third principal component	1.21	13.46	89.89	0.32	0.21	0.06	−0.13	−0.08	−0.15	0.67	0.04	−0.76
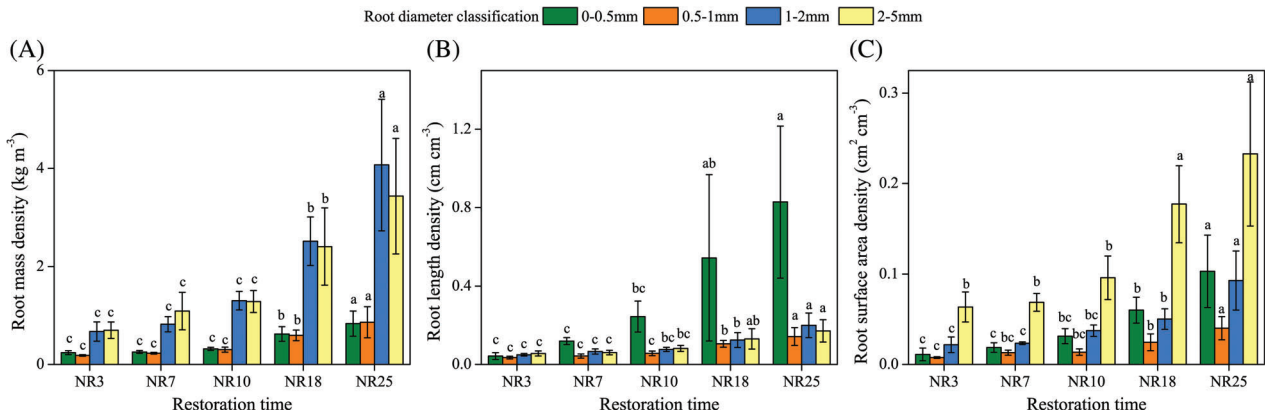
Figure 5. Changes in root characteristics at different sites. (A) Root mass density, (B) root length density, and (C) root surface area density. SF refers to slope farmland. NR3, NR7, NR10, NR18, and NR25 represent 3, 7, 10, 18, and 25 years, respectively, of passive restoration. Different lowercase letters in the same color column indicate a significant difference in root characteristics among different restoration times ($p < 0.05$). Error bars represent ±SE.

OMC, WSA, and MWD were larger than those of the other four variables (Table 2). The silt content had positive weights on PC2, whereas the clay and sand contents had negative weights, and the contribution rates of sand, silt, and clay to PC2 were much larger than that of other variables (Table 2).

Figure 4B shows that the SPI significantly increased with increasing restoration time ($p < 0.05$). However, no differences were found between NR10 and NR18 and between NR3 and NR10. The SPIs of five grasslands were 0.66, 0.82, 1.15, 1.41, and 1.94 times greater than that of SF, which further confirmed the effectiveness of vegetation restoration in improving soil properties.

Root Characteristics

Significant differences were observed in RMD, RLD, and RSAD among five grasslands (Fig. 5). For RMD, we found that RMDs of four root diameters showed no changes in the first 10 years and then increased significantly (Fig. 5A). The RLDs of 0.5–1.0, 1.0–2.0, and 2.0–5.0 mm showed a gradual increasing trend with restoration time. However, the RLD of 0–0.5 mm rapidly increased after 3-year restoration, and the RLD of 0–0.5 mm in NR7, NR10, NR18 and NR25 was 1.81–2.78, 2.99–4.33, 4.17–5.17, and 4.15–5.81 times greater than those of the other three root diameters, respectively (Fig. 5B). The RSADs of four root diameters did not change in the first 10 years (Fig. 5C). The roots of 2.0–5.0 mm had the maximum RSAD, and were 2.93–8.38, 2.93–5.28, 2.57–7.06, 2.95–7.25, and 2.26–5.81 times greater than that of the other three root diameters.

Soil Resistance to Concentrated Flow Erosion

Figure 6 shows that SRC significantly increased in the first 18 years ($p < 0.05$) and then gradually stabilized. Significant difference in SRC was not observed between NR18 and NR25. The SRCs of five restored grasslands were 1.60, 3.22, 4.68, 7.28, and 8.26 times greater than that of SF, respectively. Regression analysis indicated that change in SRC with restoration time can
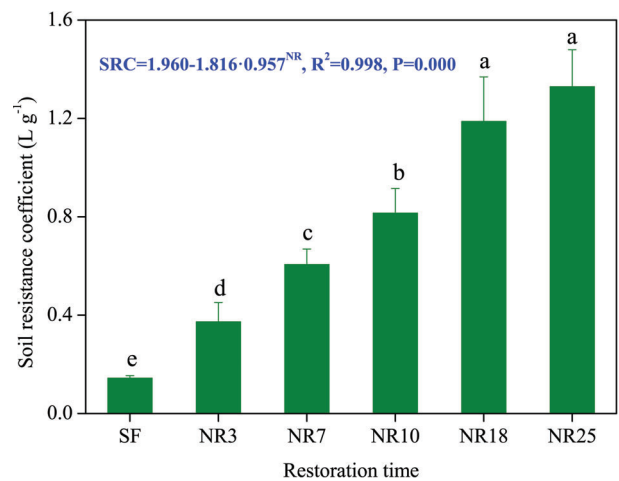

Figure 6. Variation in soil resistance coefficient (SRC) in grasslands with passive restoration time. SF refers to slope farmland. NR3, NR7, NR10, NR18, and NR25 represent 3, 7, 10, 18, and 25 years, respectively, of passive restoration. Different lowercase letters indicate a significant difference in SRC among different restoration times ($p < 0.05$). Error bars represent ±SE.

be described by an exponential function ($p = 0.000$). The results confirmed the importance of vegetation restoration in improving soil resistance to concentrated flow erosion.

Relationships Between Soil Resistance and Influencing Factors

Correlation analysis showed that SRC was positively correlated with SHC, OMC, WAS, and MWD and negatively correlated with SBD and SDR ($p < 0.01$, Fig. S1), wherein OMC had the highest correlation with SRC. Furthermore, SRC decreased by a linear and logarithmical function with SBD and SDR (Fig. S2A & S2B), respectively, while SRC increased logarithmically with SHC (Fig. S2C), increased linearly with OMC (Fig. S2D), increased exponentially with WSA (Fig. S2E), and increased by a power function with MWD (Fig. S2F).

Table 3. Fitted parameters of the hill curve for simulating the relationships between soil resistance coefficient and root density.

| Root characteristic parameter | Root diameter (mm) | Fitted Parameters | | | | Determination Coefficient |
		K	a	b	b^(1/a)	r^2
Root mass density (kg/m^3)	0–0.5	1.527	2.279	0.079	0.328	0.922
	0.5–1.0	1.470	2.231	0.057	0.277	0.970
	1.0–2.0	1.708	1.368	1.609	1.416	0.937
	2.0–5.0	1.711	1.588	1.785	1.440	0.949
Root length density (cm/cm^3)	0–0.5	1.975	0.742	0.416	0.307	0.922
	0.5–1.0	1.752	1.600	0.013	0.066	0.924
	1.0–2.0	1.511	2.444	0.002	0.079	0.936
	2.0–5.0	1.555	2.305	0.003	0.080	0.857
Root surface area density (cm^2/cm^3)	0–0.5	2.030	0.903	0.062	0.046	0.899
	0.5–1.0	1.794	1.407	0.003	0.016	0.891
	1.0–2.0	1.655	1.726	0.003	0.035	0.846
	2.0–5.0	1.658	1.779	0.017	0.101	0.912

Table 4. Path analysis of the response variable (soil resistance coefficient, SRC) and explanatory variables (soil disintegration rate, SDR; saturated hydraulic conductivity, SHC; and root mass density of 0.5–1.0 mm, RMD of 0.5–1.0 mm) with unfolding of phenotypic correlations into components of direct and indirect effects. ** Significant at $p < 0.01$.

| Explanatory variable | Correlation between SRC and explanatory variable | Direct path coefficient | Indirect Path Coefficient | | | Integrated indirect path coefficient | Integrated path coefficient |
			SDR	SHC	RMD of 0.5–1.0 mm		
SDR	−0.898**	−0.400	—	−0.166	−0.332	−0.498	−0.898
SHC	0.817**	0.232	0.287	—	0.347	0.643	0.875
RMD of 0.5–1.0 mm	0.900**	0.431	0.308	0.187	—	0.495	0.926

The relationships between SRC and RMD, RLD and RSAD of four root diameters fitted by the Hill curve (Eq. (5)) are shown in Table 3 and Fig. S3. The Hill curve simulated SRC relatively well with high determination coefficient ($r^2 = 0.846$–0.970, Table 3). SRC rapidly increased when the RMD, RLD, and RSAD of the four root diameters were lower in the initial restoration stage and generally stabilized with increasing root density (Fig. S3). Furthermore, SRC can increase by 50% when the b^(1/a) values (i.e. RMD) at diameters of 0–0.5, 0.5–1.0, 1.0–2.0, and 2.0–5.0 mm increase from 0 to 0.328, 0.277, 1.416, 1.440 kg/m^3, respectively (Table 3; Fig. S3A). Roots of 0.5–1.0 mm correspond to the lowest b^(1/a) value, indicating that the low RMD of 0.5–1.0 mm can achieve a targeted increase in SRC (50%) better than the other three root diameters. For RLD and RSAD, the minimum b^(1/a) values were 0.066 cm/cm^3 and 0.016 cm^2/cm^3, respectively, which also correspond to the 0.5–1.0 mm diameter (Table 3).

A stepwise regression (forward) was performed to determine the optimal soil and root factors influencing SRC. The results showed that the multiple regression model (Eq. (6)) had the highest efficiency when SDR, SHC, and RMD of 0.5–1.0 mm were included.

$$SRC = 0.554RMD + 1.512SHC - 0.365SDR$$
$$+ 0.725 \; (r^2 = 0.937, N = 20, p < 0.001) \quad (6)$$

Pearson correlation analysis showed significant correlations among RMD, SDR, and SHC (Table 4), and changes in any one of the three variables would cause changes in the other two variables. Therefore, path coefficients were used to determine the direct and indirect effects of the three variables on SRC. Table 4 shows that RMD had the greatest direct effects (0.431) followed by SDR (−0.40) and SHC (0.232). In terms of indirect effects, SDR exerted a higher indirect effect (−0.332) on SRC via RMD than SHC (−0.166), and the indirect effects of SHC on SRC via SDR or RMD were 0.287 and 0.347, respectively. Overall, SHC had the highest integrated indirect effects (0.643) followed by SDR (−0.498) and RMD (0.495), and the three explanatory variables contributed to higher indirect effects than direct effects. Finally, the highest integrated effect was found for RMD (0.926), SDR (−0.898), and SHC (0.875).

Discussion

Effect of Vegetation Restoration on Soil Properties

Temporal changes in soil properties reflect the effectiveness of vegetation restoration (Jiao et al. 2010; Ashwood et al. 2019). Our results show that soil particle distribution did not change with vegetation succession, indicating that soil texture was mainly inherited from parent materials and difficult to change (Li & Shao 2006). Our results also show that SBD, SHC, OMC, WSA, and MWD increased while SDR decreased with increasing duration of restoration, which is consistent with previous

findings (Li & Shao 2006; Zhao et al. 2013). During revegetation, the varied plant species along successional time inevitably affect soil properties because of the differences in plant aboveground biomass and root biological functions (Hok et al. 2015). In this study, SHC and soil resistance to disintegration significantly increased with increasing restoration time, which was mainly due to the improvement in root physical binding and bonding effects (Li et al. 2015). Specifically, soil WSAs tend towards stability after a 7-year restoration timeframe, which is basically consistent with the finding of Zhao et al. (2013), who reported WSA greater than 0.25 mm did not change after 6-year restoration. This finding further demonstrates the effectiveness of vegetation restoration and its ability to quickly stabilize soil structure. There are two essential reasons for the above results. First, fresh plant residues and root exudates in soil and root surface and decomposed root residues in subsurface soil can be directly transformed into soil organic matter (Zhu et al. 2010; Zhao et al. 2013), can provide energy/carbon sources and nutrients for soil microorganisms (Zhu et al. 2010), and can promote the formation of WSAs (Six et al. 2004). Second, significant improvements in root density during revegetation can cause an increase in organic matter inputs, such as litter and dead roots in the soil (Peichl et al. 2012; Prietzel & Bachmann 2012), and thus improve the OMC. However, for SF, the cultivation and harvest of crops restricts the return of nutrients to soil, which is not conducive to the formation of better soil properties (Wang et al. 2017). Thus, the increase in soil nutrition following the conversion of SF to restored grasslands was confirmed to have positive effects on soil properties. Moreover, the SPI significantly increased with increasing restoration time, further indicating the important role of vegetation restoration in improving soil quality. From the above discussion, the changes in soil properties with restoration time suggest that revegetation is an effective approach to improve soil properties and restore soil ecology (Jiao et al. 2010; Wortley et al. 2013).

Response of Soil Resistance to Soil Properties

The ultimate goal of vegetation restoration is to improve the soil resistance to concentrated flow erosion (SRC) of the Loess Plateau. Our study revealed that SRC was significantly improved by revegetation and was positively correlated with SBD, SHC, OMC, WAS, and MWD and negatively correlated with SDR ($p < 0.01$). This result indicated that the increase of SRC with restoration time was strongly related to the improvement in soil properties induced by revegetation (Li et al. 2017; Zhang et al. 2017). As the restoration time increased, more roots became interwoven into soil body, which improved soil OMC, promoted soil microorganism activity and the formation of WSAs, thereby increasing soil permeability (Wu et al. 2000). Thus, a higher OMC and more stable aggregate structure can reinforce soil resistance to concentrated flow erosion (Li et al. 2017; Zhang et al. 2017). In addition, more roots can enhance the root binding and bonding effects that can increase soil resistance to water disintegration (Li et al. 2015; Guo et al. 2018), which is also the reason why the SRC decreases with

increasing SDR (Li et al. 2017; Wang & Zhang 2017). However, Wang et al. (2014, 2018) reported that OMC and WSA had no significant effect on soil detachment by overland flow. On the one hand, this pattern is probably due to the relatively small variations in OMC and WSA among different restoration models and/or SBD and soil cohesion having much stronger effects on soil detachment (Wang et al. 2014, 2018). On the other hand, differences in vegetation types between this study and their studies induced by different succession processes can result in distinctly different effects on soil resistance to concentrated flow erosion (Feng et al. 2018; Wang et al. 2018). From the above discussion, the positive relationships between soil resistance and soil properties indicate that passive vegetation restoration can be confirmed as a meaningful measure to control soil erosion and improve the ecological environment on the Loess Plateau.

Response of Soil Resistance to Root Characteristics

Our results revealed that the relationships between SRC and root density of different diameters were well simulated by the Hill curve. The improvement in SRC is clearly enhanced by roots of different diameters, as supported by previous studies (De Baets et al. 2006; Wang et al. 2014; Li et al. 2015; Wang et al. 2018). We found that SRC rapidly increased when root density was low, indicating the vital role of root systems in improving soil SRC, although root density was low in the initial stage of vegetation restoration (Li et al. 1992). However, SRC generally stabilized with increasing root density, which suggests that a greater root density was not necessary and a proper and low root density could optimally improve SRC in view of the lack of water resources in the Loess Plateau (Feng et al. 2012).

Furthermore, the value of $b^\wedge(1/a)$ was used to evaluate which diameter roots have higher effectiveness in improving soil erosion resistance (Li et al. 1991). Our results showed that for RMD, RLD, and RSAD, the minimum $b^\wedge(1/a)$ values were 0.277 kg/m^3, 0.066 cm/cm^3, and 0.016 cm^2/cm^3, respectively, which all correspond to the 0.5–1.0 mm diameter roots. This result further indicated that fine roots had a stronger effect on flow erosion than roots with greater diameters, as supported by Li et al. (1991, 1992) and Wu et al. (2000), who reported that fine roots had the greatest effect on SRC in the Loess Plateau and in the red soil region of southern China, respectively. However, De Baets et al. (2006) reported $b^\wedge(1/a)$ values for RMD of 0.79 kg/m^3, and the value was greater than those of this study. This difference is mainly due to the difference in plant species and root architectures causing different erosion control benefits (De Baets et al. 2007; Wang et al. 2014; Feng et al. 2018). Considering that the minimum $b^\wedge(1/a)$ value was found at the same root diameter (0.5–1.0 mm) for RMD, RLD, and RSAD, to determine which root index had the highest effect on SRC, the optimal relationships among the RMD, RLD, and RSAD are fitted and shown as Eqs. (7) and (8). Based on the two equations, when the RMD of 0.5–1.0 mm is 0.277 kg/m^3, the RLD and RSAD are 0.0512 cm/cm^3 and 0.0132 cm^2/cm^3, respectively, and were lower than the $b^\wedge(1/a)$

values of $0.066\,\mathrm{cm/cm^3}$ and $0.016\,\mathrm{cm^2/cm^3}$. This result indicated that an RMD of $0.5–1.0\,\mathrm{mm}$ is the most effective root diameter for improving soil SRC:

$$\mathrm{RLD}_{0.5–1.0\ \mathrm{mm}} = 0.166\mathrm{RMD}_{0.5–1.0\ \mathrm{mm}}^{0.917}$$
$$(r^2 = 0.932, N = 20, p < 0.001) \qquad (7)$$

$$\mathrm{RSAD}_{0.5–1.0\ \mathrm{mm}} = 0.044\mathrm{RMD}_{0.5–1.0\ \mathrm{mm}} + 0.001$$
$$(r^2 = 0.938, N = 20, p < 0.001) \qquad (8)$$

In addition, our results revealed that SDR, SHC, and RMD of $0.5–1.0\,\mathrm{mm}$ were the key factors influencing SRC. Moreover, the RMD of $0.5–1.0\,\mathrm{mm}$ had the greater direct effects on SRC than SDR and SHC based on the path analysis, which further highlights that roots had a relatively strong influence on SRC and suggests that vegetations rich in $0.5–1.0\,\mathrm{mm}$ roots should be preferred in vegetation restoration practice.

In conclusion, our study reveals that soil properties and root density gradually improved and that the SRC increased significantly by $1.60–8.26$ times along a 25-year passive succession from farmland to grasslands. The enhancement of SRC was positively related to the improvement of soil properties induced by revegetation, and the roots with diameters of $0.5–1.0\,\mathrm{mm}$ present a better ability to improve SRC than roots with other diameters. The RMD of $0.5–1.0\,\mathrm{mm}$, SHC, and SDR are the most critical factors influencing SRC. This study suggests that vegetations rich in $0.5–1.0\,\mathrm{mm}$ roots should be preferred during revegetation practice, and an appropriate and low root density should also be considered in view of the water shortage on the Loess Plateau.

Acknowledgments

LITERATURE CITED

Ashwood F, Watts K, Park K (2019) Woodland restoration on agricultural land: long-term impacts on soil quality. Restoration Ecology https://doi.org/10.1111/rec.13003

De Baets S, Poese J, Gyssels G, Knapen A (2006) Effects of grass roots on the erodibility of topsoils during concentrated flow. Geomorphology 76:54–67

De Baets S, Poesen J, Knapen A, Galindo P (2007) Impact of root architecture on the erosion-reducing potential of roots during concentrated flow. Earth Surface Processes and Landforms 32:1323–1345

Feng X, Sun G, Fu B, Su C, Liu Y, Lamparski H (2012) Regional effects of vegetation restoration on water yield across the Loess Plateau, China. Hydrology and Earth System Sciences 16:2617–2628

Feng TJ, Wei W, Chen LD, Jesús R, Die C, Feng XR, Ren KM, Brevik EC, Yu Y (2018) Assessment of the impact of different vegetation patterns on soil erosion processes on semiarid loess slopes. Earth Surface Processes and Landforms 43:1860–1870

Fu BJ, Chen LD, Ma KM, Zhou HF, Wang J (2000) The relationships between land use and soil conditions in the hilly area of the Loess Plateau in northern Shaanxi, China. Catena 39:69–78

Fu BJ, Liu Y, Lu YH, He CS, Zeng Y, Wu BF (2011) Assessing the soil erosion control service of ecosystems change in the Loess Plateau of China. Ecological Complexity 8:284–293

Guo MM, Wang WL, Kang HL, Yang B (2018) Changes in soil properties and erodibility of gully heads induced by vegetation restoration on the Loess Plateau, China. Journal of Arid Land 10:712–725

Gyssels G, Poesen J (2010) The importance of plant root characteristics in controlling concentrated flow erosion rates. Earth Surface Processes and Landforms 28:371–384

Hok L, de Moraes Sa JC, Boulakia S, Reyes M, Leng V, Kong R, et al. (2015) Short-term conservation agriculture and biomass-C input impacts on soil C dynamics in a savanna ecosystem in Cambodia. Agriculture, Ecosystems and Environment 214:54–67

Hu W, Shao MA, Wang QJ, Fan J, Horton R (2009) Temporal changes of soil hydraulic properties under different land uses. Geoderma 149:355–366

Jiang DS, Li XH, Fan XK, Zhang HX (1995) Research on the law of soil disintegration rate change and its effect factors on the Loess Plateau. Journal of Soil and Water Conservation 15:20–27 (in Chinese)

Jiao JY, Tzanopoulos J, Xofis P, Mitchley J (2008) Factors affecting distribution of vegetation types on abandoned cropland in the hilly-gullied Loess Plateau region of China. Pedosphere 18:24–33

Jiao J, Zhang Z, Bai W, Jia Y, Wang N (2010) Assessing the ecological success of restoration by afforestation on the Chinese Loess Plateau. Restoration Ecology 20:240–249

Kou M, Jiao J, Yin Q, Wang N, Wang Z, Li Y (2016) Successional trajectory over 10 years of vegetation restoration of abandoned slope croplands in the hill-gully region of the Loess Plateau. Land Degradation & Development 27:919–932

Li YY, Shao MA (2006) Change of soil physical properties under long-term natural vegetation restoration in the Loess Plateau of China. Journal of Arid Environments 64:77–96

Li Y, Zhu XM, Tian JY (1991) Effectiveness of plant roots to increase the anti-scouribility of soil on the Loess Plateau. Chinese Science Bulletin 36:2077–2082

Li Y, Xu XQ, Zhu XM (1992) Preliminary study on mechanism of plant-roots to increase soil anti-scouribility on the Loess Plateau. Science in China. Series B 35:1085–1092

Li P, Li ZB, Tan TZ (2005) Dynamic distribution characters of herbaceous vegetation root systems in abandoned grasslands of Loess Plateau. Chinese Journal of Applied Ecology 16:849–853 (in Chinese)

Li Q, Liu GB, Zhang Z, Tuo DF, Xu MX (2015) Effect of root architecture on structural stability and erodibility of topsoils during concentrated flow in hilly Loess Plateau. Chinese Geographical Science 25:757–764

Li JJ, Li Z, Lu ZM (2016) Analysis of spatiotemporal variations in land use on the Loess Plateau of China during 1986–2010. Environment and Earth Science 75:997

Li Q, Liu GB, Zhang Z, Tuo DF, Bai RR, Qiao FF (2017) Relative contribution of root physical enlacing and biochemistrical exudates to soil erosion resistance in the loess soil. Catena 153:61–65

Liang MY, Liu XC, Zeng JQ, Wang T (2010) The investigation and evaluation of the natural vegetation in Dongzhi Plateau, eastern Gansu Province. Ecological Science 29:351–357 (in Chinese)

Mamo M, Bubenzer GD (2001) Detachment rate, soil erodibility and soil strength as influenced by plant roots. Part 2. Field study. Transactions of ASAE 44:1175–1181

Peichl M, Leava NA, Kiely G (2012) Above- and below-ground ecosystem biomass, carbon and nitrogen allocation in recently afforested grassland and adjacent intensively managed grassland. Plant and Soil 350:281–296

Prietzel J, Bachmann S (2012) Changes in soil organic C and N stocks after forest transformation from Norway spruce and Scots pine into Douglas fir, Douglas fir/spruce, or European beech stands at different sites in southern Germany. Forest Ecology and Management 269:134–148

Six J, Bossuyt H, Degryze S, Denef K (2004) A history of research on the link between (micro)aggregates, soil biota, and soil organic matter dynamics. Soil & Tillage Research 79:7–31

Vannoppen W, Vanmaercke M, Baets SD, Poesen J (2015) A review of the mechanical effects of plant roots on concentrated flow erosion rates. Earth-Science Reviews 150:666–678

Wang B, Zhang GH (2017) Quantifying the binding and bonding effects of plant roots on soil detachment by overland flow in 10 typical grasslands on the Loess Plateau. Soil Science Society of America Journal 81:1567–1576

Wang B, Zhang GH, Shi YY, Zhang XC (2014) Soil detachment by overland flow under different vegetation restoration models in the Loess Plateau of China. Catena 116:51–59

Wang B, Zhang GH, Shi YY, Li ZW, Shan ZJ (2015) Effects of near soil surface characteristics on the soil detachment process in a chronological series of vegetation restoration. Soil Science Society of America Journal 79:1213–1222

Wang J, Wang P, Qin Q, Wang H (2017) The effects of land subsidence and rehabilitation on soil hydraulic properties in a mining area in the Loess Plateau of China. Catena 159:51–59

Wang B, Zhang GH, Yang YF, Li PP, Liu JX (2018) Response of soil detachment capacity to plant root and soil properties in typical grasslands on the Loess Plateau. Agriculture, Ecosystems and Environment 266:68–75

Wortley L, Hero JM, Howes M (2013) Evaluating ecological restoration success: a review of the literature. Restoration Ecology 21:537–543

Wu WD, Zheng SZ, Lu ZH, Zhang TL (2000) Effect of plant roots on penetrability and anti-scouribility of red soil derived from granite. Pedosphere 10:183–188

Wu GL, Liu Y, Fang NF (2016) Soil physical properties response to grassland conversion from cropland on the semiarid area. Ecohydrology 9:1471–1479

Yu YC, Zhang GH, Geng R, Sun L (2014) Temporal variation in soil detachment capacity by overland flow under four typical crops in the Loess Plateau of China. Biosystems Engineering 122:139–148

Zhang GH (2017) Uncertainty analysis of soil detachment capacity measurement. Journal of Water and Soil Conservation 31:1–6 (in Chinese)

Zhang Z, Li Q, Liu G (2017) Soil resistance to concentrated flow and sediment yields following cropland abandonment on the Loess Plateau, China. Journal of Soils and Sediments 17:1–10

Zhao AC (1994) Analysis of control models of typical small watershed in gully area of Loess Plateau, the east part of Gansu Province. Research of Soil and Water Conservation 1:45–49 (in Chinese)

Zhao Y, Wu P, Zhao S, Feng H (2013) Variation of soil infiltrability across a 79-year chronosequence of naturally restored grassland on the Loess Plateau, China. Journal of Hydrology 504:94–103

Zhou ZC, Gan ZT, Shangguan ZP, Dong ZB (2010) Effects of grazing on soil physical properties and soil erodibility in semiarid grassland of the northern Loess Plateau (China). Catena 82:87–91

Zhu BB, Li ZB, Li P (2010) Soil erodibility, microbial biomass, and physical–chemical property changes during long-term natural vegetation restoration: a case study in the loess plateau, China. Ecological Research 25:531–541

Supporting Information

The following information may be found in the online version of this article:

Figure S1. Correlation matrix among the soil resistance coefficient and soil properties.
Figure S2. Relationships between the soil resistance coefficient and soil properties.
Figure S3. Relationships between the soil resistance coefficient and root density for roots of different diameters.